# Olefin Cyclopropanation Catalyzed by Iridium(III) Porphyrin Complexes

Bernie J. Anding, Arkady Ellern, and L. Keith Woo*

Department of Chemistry, Iowa State University, Ames, Iowa 50011-3111, United States

**S** *Supporting Information*

**ABSTRACT:** Tetratolylporphyrinato (TTP) iridium complexes were shown to be extremely active and robust catalysts for the cyclopropanation of olefins using diazo compounds as carbene sources. Ir(TTP)CH$_3$ (**1**) catalyzed the cyclopropanation of styrene with ethyl diazoacetate (EDA) at −78 °C and achieved 4.8 × 10$^5$ turnovers in three successive reagent additions with no sign of deactivation. High yields and moderate trans selectivities were attained for electron-rich and sterically unhindered substrates. A Hammett $\rho^+$ value of −0.23 was determined by competition experiments with para-substituted styrenes. Furthermore, competitive cyclopropanation of styrene and styrene-$d_8$ with EDA and **1** demonstrated a moderate inverse secondary isotope effect of 0.86 ± 0.03. These data are consistent with a catalytic cycle that proceeds through a metalloporphyrin carbene intermediate. Carbene transfer to olefin substrates appears to be rate limiting, as indicated by kinetic studies. Hexavalent iridium halogenato tetratolylporphyrinato complexes of the form Ir(TTP)X(L), where X = Cl, Br, I, NCS and L = CO, NMe$_3$ (**2−6**), and cationic analogues, where X = BF$_4$ and L = CO or vacant site (**7**, **8**), also demonstrated high catalytic cyclopropanation activity.
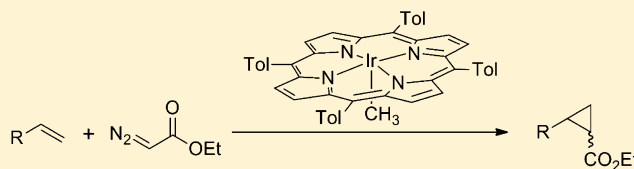
## INTRODUCTION

Over the past few decades, carbene transfer reactions used to generate new C−C bonds have grown tremendously in synthetic utility.[1−3] Furthermore, carbene moieties generated from diazo reagents provide attractive atom-efficient and environmentally friendly protocols, because N$_2$ is the only byproduct. Although many diazo reagents react sluggishly on their own, various catalysts efficiently assist in the formation of carbene intermediates.[4−7] Among the highly active and robust catalysts, metalloporphyrin complexes are particularly versatile for the design of stereoselective carbene transfers.[8−10] Metalloporphyrins containing iron,[11] ruthenium,[12] osmium,[13] cobalt,[14,15] and rhodium[15] are all active for catalytic carbene transfer. For example, Fe and Rh complexes, exhibit a great breadth of catalytic range, including C−H insertions,[10,16] N−H insertions,[17] olefinations,[18] and cyclopropanations.[11,19] In addition, iron porphyrin catalysts are robust enough to achieve 4300 turnovers,[20] and rhodium adducts furnish cyclopropanation and C−H insertion products with unusual selectivity for *cis*-cyclopropanes and primary insertion products, respectively.[21,22] Despite these notable results for group 8 and group 9 metals, the reactivity of iridium porphyrins toward carbene transfer has not been reported.

Examples of catalysis by halogenato iridium porphyrins are quite rare in comparison to those for the related rhodium porphyrins. This may be due, in part, to the presence of a kinetically inert CO ligand bound to iridium analogues, yielding a hexavalent complex devoid of an available vacant site.[23] Indeed, the mechanism of cyclopropanation by Rh(TTP)I, reported by Kodadek and co-workers, requires an open site for the initial coordination of the diazo compound (Scheme 1).[24]

**Scheme 1. Cyclopropanation Mechanism for Rh(TTP)I**
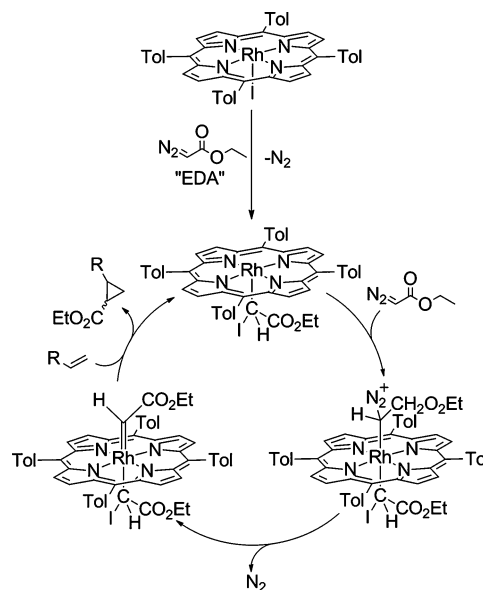


Interestingly, the active catalyst was believed to exist primarily as an alkylrhodium complex resulting from initial carbene insertion into the Rh−I bond. Analogous alkyliridium porphyrin compounds, unlike their halogenato counterparts, are pentacoordinate species that appear to be good candidates for catalysis. The present work explores the catalytic activity of
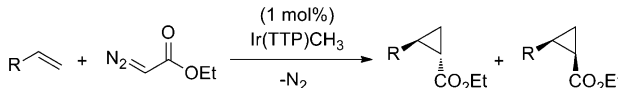
alkyliridium porphyrin complexes, as well as other iridium(III) porphyrins, toward transformations with diazo reagents. The work described herein serves as the first examples of carbene transfer catalyzed by iridium porphyrin complexes.

### ■ RESULTS AND DISCUSSION

The catalytic cyclopropanation activity of both methyl and halogenato iridium tetratolylporphyrinato (TTP) complexes, Ir(TTP)CH₃ (**1**) and Ir(TTP)Cl(CO) (**2**) were evaluated. Syntheses of these complexes were reported previously.[25,26] Preliminary reactivity studies showed that methyliridium complex **1** decomposed ethyl diazoacetate (EDA) readily at temperatures as low as −78 °C to form maleates and fumarates (cis:trans = 6.5:1) in quantitative yield. Reaction intermediates were too transient for spectroscopic observation by ¹H NMR. With these initial results, the cyclopropanation of various olefins and EDA using **1** was explored using a protocol similar to that developed for *N,N′*-bis(salicylidene)ethylenediiminato iridium, Ir(salen).[27] Dropwise addition of EDA to a solution of styrene and **1** at room temperature resulted in instantaneous gas evolution. Cyclopropanes were formed in 35% yield along with a significant amount of dimerization of the diazo reagent to form diethyl maleate and diethyl fumarate (Table 1). The

**Table 1. Cyclopropanation of EDA and Alkenes with Ir(TTP)CH₃[a]**

| substrate | solvent | time (min) | $T$ (°C) | yield (%)[b] | trans:cis[b] |
|---|---|---|---|---|---|
| styrene | CH₂Cl₂ | <5 | 23 | 35 | 5.5:1 |
| styrene | CH₂Cl₂ | <5 | −78 | 85 | 5.8:1 |
| styrene | THF | 30 | 0 | 80 | 6.3:1 |
| 4-methoxystyrene | CH₂Cl₂ | <5 | −78 | 86 | 3.4:1 |
| 4-methylstyrene | CH₂Cl₂ | <5 | −78 | 84 | 5.8:1 |
| 4-bromostyrene | CH₂Cl₂ | <5 | −78 | 91 | 7.3:1 |
| 4-nitrostyrene[c] | CH₂Cl₂ | <5 | −78 | 84 | 8.0:1 |
| α-methylstyrene | CH₂Cl₂ | <5 | −78 | 90 | 2.0:1 |
| 1-hexene | CH₂Cl₂ | 20 | −78 | 60 | 3.3:1 |
| indene | CH₂Cl₂ | 30 | −78 | 62 | 3.2:1 |
| cyclohexene | CH₂Cl₂ | <5 | 23 | 14[d] | e |
| trans-β-methylstyrene | CH₂Cl₂ | <5 | 23 | 31[d] | 1[f] |
| ethyl acrylate | CH₂Cl₂ | <5 | 23 | 12[d] | ~10:1 |

[a]Conditions: 1 × 10⁻³ M in Ir(TTP)CH₃; Ir(TTP)-CH₃:EDA:substrate = 1:100:500. [b]Yields and diastereomeric ratios of cyclopropanes as determined by GC. [c]4-Nitrostyrene was not distilled prior to use. [d]Determined by NMR. [e]Isomer not determined. [f]Only one isomer observed.

sum of the yields for cyclopropanation and dimerization correspond to complete conversion of EDA. Lowering the reaction temperature to −78 °C resulted in a significant increase in yield for cyclopropanes (85%), with a corresponding decrease in dimerization of the diazo reagent. This method was cleanly extended to other terminal aryl olefins. In contrast, electron-deficient and internal olefins (except indene) required longer reaction times or higher temperatures. Yields for these substrates were lower, especially for those run at room temperature, where dimerization becomes dominant. This

method was also applicable to less reactive diazo reagents such as methyl 2-phenyldiazoacetate (MPDA; eq 1).
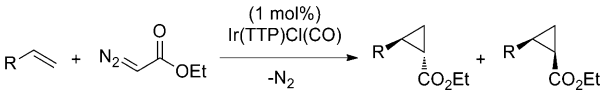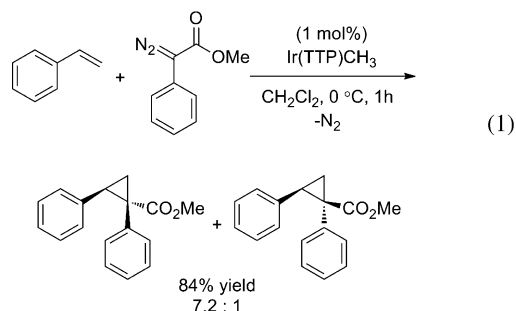
Reactions catalyzed by **1** displayed a moderate preference for trans cyclopropanes. This selectivity was enhanced slightly for reactions run in THF, albeit at higher temperatures and longer reaction times. In comparison to similar catalysts, **1** was more trans selective than Rh(TPP)I but less than Fe(TPP)Cl.[20,21] Moreover, analysis of the diastereoselectivity for the para-substituted styrenes revealed an influence of substrate electronics on diastereoselectivity. Substrates with electron-withdrawing groups at the para position displayed a larger preference for trans cyclopropanes. Notably, cyclopropanation with *trans-β*-methylstyrene formed only the isomer bearing the phenyl group anti to both methyl and ethyl carboxylate, as determined by NOESY.

To evaluate catalyst activity further, cyclopropanation was explored at very low catalyst loadings. Using 5.8 × 10⁻⁴ mol % of **1** relative to EDA in the presence of excess styrene, diazo conversion and cyclopropanation of styrene were determined after warming the reaction mixture to room temperature from −78 °C. For three consecutive diazo additions, EDA was quantitatively consumed to form cyclopropanes with a small amount of diazo dimerization. Cyclopropanation yields were 93%, 92%, and 91% for the first, second, and third additions, respectively. Overall, **1** achieved 4.8 × 10⁵ turnovers with almost no indication of catalyst deactivation. This TON is nearly 2 orders of magnitude greater than the values reported for Ru and Rh porphyrin catalysts.[28−30]

Surprisingly, Ir(TTP)Cl(CO) (**2**) also effectively catalyzed the cyclopropanation of olefins with EDA, despite being coordinatively saturated (Table 2). The substrate reactivity trends were similar for both **1** and **2**. However, **2** required higher reaction temperatures and longer reaction times. Although **2** was less selective for trans cyclopropane products, it was slightly more efficient for the cyclopropanation of more hindered and electron-deficient olefins.

Various metalloporphyrin complexes, of the form [Ir(TTP)-(L)]⁺ or Ir(TTP)X(L), where X is an anionic ligand and L is a neutral ligand, were generated to compare axial ligand effects on catalytic activity. CO ligand substitution was accomplished by adding trimethylamine *N*-oxide to a CH₂Cl₂ solution of **2** (Scheme 2). The resulting product was established to be Ir(TTP)Cl(NMe₃) (**3**) on the basis of ¹H NMR and IR spectroscopy. Protons of the axially coordinated NMe₃ were strongly shifted upfield due to the porphyrin ring current effect and appeared as a sharp singlet at −2.99 ppm. Moreover, CO loss was verified by the disappearance of the strong Ir−C≡O stretch at 2050 cm⁻¹. The molecular structure of **3** (Figure 1) was determined by single-crystal X-ray analysis. One molecule of **3** occupied the asymmetric unit of the monoclinic cell

**Table 2. Cyclopropanation of EDA and Alkenes with Ir(TTP)Cl(CO)[a]**



| substrate | solvent | time (min) | $T$ (°C) | yield (%)[b] | trans:cis[b] |
|---|---|---|---|---|---|
| styrene | CH$_2$Cl$_2$ | <5 | 23 | 92 | 4.7:1 |
| styrene | CH$_2$Cl$_2$ | 20 | 0 | 85 | 4.9:1 |
| styrene | THF | 90 | 23 | 75 | 4.3:1 |
| $\alpha$-methylstyrene | CH$_2$Cl$_2$ | 20 | 0 | 93 | 1.8:1 |
| 1-hexene | CH$_2$Cl$_2$ | 30 | 0 | 59 | 3.5:1 |
| indene | CH$_2$Cl$_2$ | 60 | 0 | 43 | 2.5:1 |
| cyclohexene | CH$_2$Cl$_2$ | <5 | 23 | 20[c] | d |
| trans-$\beta$-methylstyrene | CH$_2$Cl$_2$ | <5 | 23 | 67[c] | 1[e] |
| ethyl acrylate | CH$_2$Cl$_2$ | <5 | 23 | 24 | ~10:1 |

[a]Conditions: 1 × 10$^{-3}$ M in Ir(TTP)Cl(CO); Ir(TTP)Cl-(CO):EDA:substrate = 1:100:500. [b]Yields and diastereomeric ratios of cyclopropanes as determined by GC. [c]Determined by NMR. [d]Isomer not determined. [e]Only one isomer observed.

**Scheme 2. Synthesis of Complexes of the form Ir(TTP)X(L)**
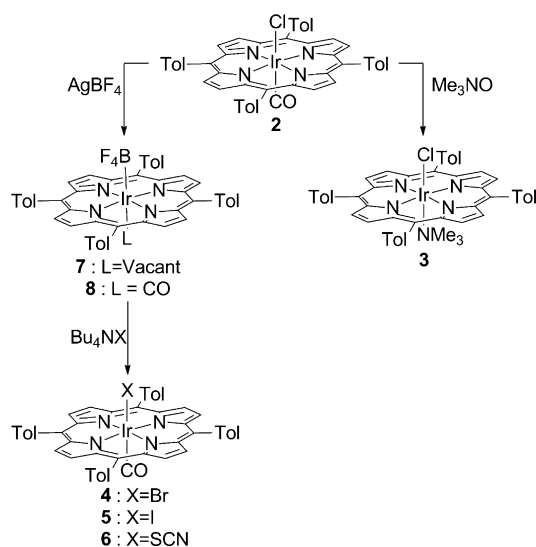


together with two molecules of CH$_2$Cl$_2$. Presumably, oxidization of CO to CO$_2$ by trimethylamine *N*-oxide generated a pentacoordinate chloroiridium complex, which was quickly trapped by the in situ generated trimethylamine.[31] This
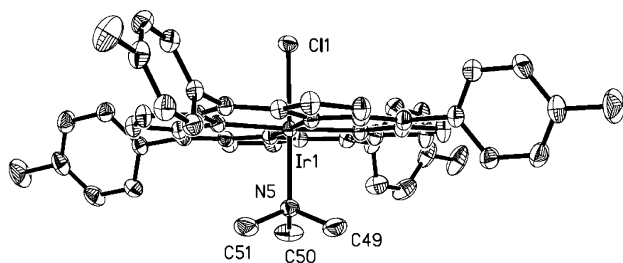


**Figure 1.** ORTEP[32] of **3** with 50% probability thermal ellipsoids. Selected bond distances (Å): average Ir(1)−N$_{pyrrole}$ = 2.035(4), Ir(1)−Cl(1) = 2.355(1), Ir(1)−N(5) = 2.174(2), average N(5)−C = 1.479(6).

represents only the second decarbonylation procedure published for Ir(TTP)Cl(CO).[23]

Anionic ligand substitution products were generated by chloride abstraction from **2** with silver(I) tetrafluoroborate, followed by anion addition with the appropriate tetrabutylammonium salt. Only minor spectroscopic differences were observed between **2** and Ir(TTP)(CO)X (**4**, X = Br; **5**, X = I; **6**, X = SCN). Compositions and molecular structures were confirmed by mass spectrometry and single-crystal X-ray analysis (Figures 2 and 3). Selected metrical parameters are
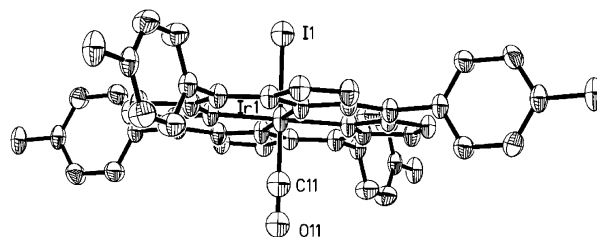


**Figure 2.** ORTEP of **5** showing one of the two configurations disordered by a mirror plane. Thermal ellipsoids are drawn at the 50% probability level. Selected bond distances (Å) and angles (deg) for **5**: Ir(1)−N = 2.048(7), Ir(1)−I(1) = 2.491(2), Ir(1)−C(11) = 1.852(2), C(11)−O(11) = 1.141(2); I(1)−Ir(1)−C(11) = 180, I(1)−Ir(1)−N$_4$(EQP) = 90, C(11)−Ir(1)−N$_4$(EQP) = 90. Selected bond distances (Å) and angles (deg) for isostructural **4**: Ir(1)−N$_{pyrrole}$ = 2.047(4), Ir(1)−Br(1) = 2.409(2), Ir(1)−C(11) = 1.855(3), C(11)−O(11) = 1.143(3); Br(1)−Ir(1)−C(11) = 180, Br(1)−Ir(1)−N$_4$(EQP) = 90, C(11)−Ir(1)−N$_4$(EQP) = 90.
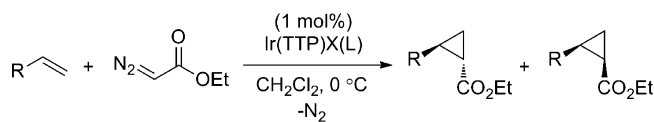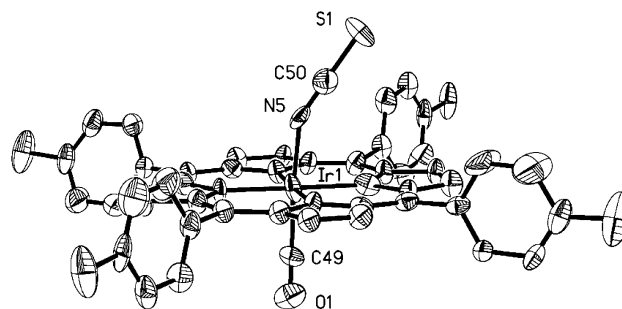


**Figure 3.** ORTEP of **6**. Thermal ellipsoids are drawn at the 50% probability level. Selected bond distances (Å): average Ir(1)−N$_{pyrrole}$ = 2.049(12), Ir(1)−N(5) = 1.961(14), N(5)−C(50) = 1.17(2), C(50)−S(1) = 1.664(19), Ir(1)−C(49) = 1.897(14), C(49)−O(1) = 1.153(17).

given in the figure captions. Complexes **4** and **5** are isostructural, and both crystallize in the *I*4/*m* space group with a fourth of the molecule in the asymmetric unit and the Ir atom in a 4/*m* site symmetry. The central Ir atom has typical octahedral coordination with an ideal Ir−N$_4$ equatorial plane (EQP) and displays axial ligand disorder through a mirror plane. For X = SCN, complex **6**, N coordination of the thioisocyanate ligand to the metal center through nitrogen was confirmed by bond length analysis. Notably, the Ir−N(CS) bond is 0.049(14) Å shorter than that for the shortest reported Ir−N(CS) compound.[33] If no anionic ligand sources were added after chloride abstraction, an inseparable mixture of cationic iridium(III) porphyrin complexes, Ir(TTP)(BF$_4$) (**7**) and Ir(TTP)(BF$_4$)(CO) (**8**), was obtained in variable ratios.[34] Attempts to cleanly isolate either of these cationic complexes failed.

Catalytic results, compiled in Table 3, show that the activity of hexavalent iridium porphyrin complexes for the cyclo-

**Table 3. Cyclopropanation of EDA and Styrene using Various Ir Porphyrin Catalysts**[a]



| cat. | time (min) | yield (%) | trans:cis |
|---|---|---|---|
| Ir(TTP)Cl(CO) (**2**) | 20 | 85 | 4.9:1 |
| Ir(TTP)Cl(NMe$_3$) (**3**) | 60 | 75 | 5.0:1 |
| Ir(TTP)Br(CO) (**4**) | 60 | 75 | 4.6:1 |
| Ir(TTP)I(CO) (**5**) | <5 | 56 | 5.5:1 |
| Ir(TTP)SCN(CO) (**6**) | 120 | 86 | 4.5:1 |
| Ir(TTP)(BF$_4$)/Ir(TTP)(BF$_4$)(CO) (**7/8**) | <5 | 93 | 3.3:1 |
| **2** and AgBF$_4$[b] | <5 | 93 | 3.0:1 |

[a]Conditions: $1 \times 10^{-3}$ M in catalyst; catalyst:EDA:styrene = 1:100:500; reactions run at 0 °C in CH$_2$Cl$_2$. Yields and diastereomeric ratios were determined by GC. [b]**2** and AgBF$_4$ were premixed in CH$_2$Cl$_2$ and stirred for 30 min.

propanation of styrene with EDA was relatively independent of the type of axial ligand. The only neutral species that showed a significant change in reactivity was Ir(TTP)I(CO). In comparison to other halogenato iridium porphyrins, Ir(TTP)-I(CO) was considerably more active and diastereoselective, but cyclopropanation yields were lower, due to increased dimerization of the diazo reagent. In contrast, the cationic catalyst mixture (**7/8**) was as reactive and efficient toward cyclopropanation, but lower diastereoselectivity was observed. The cationic catalysts were either synthesized and isolated before cyclopropanation or generated in situ with silver tetrafluoroborate. Regardless of catalyst preparation, the catalytic efficiency and selectivity were effectively unchanged.

The above results for iridium porphyrin compounds share many similarities with group 8 metalloporphyrin catalysts. Both types of catalysts are trans selective and react smoothly with terminal aryl olefins. In addition, yields decrease significantly for electron-poor or sterically hindered olefins. This reduction in efficiency was not nearly as drastic for cobalt and rhodium porphyrin catalysts.[19,35] On the basis of these observations, a mechanism similar to that previously proposed for group 8 metalloporphyrins seems likely for the catalytic pathway undertaken for cyclopropanation by Ir(TTP)CH$_3$ (Scheme 3).[20,24] The initial step involves EDA coordination to form a diazoalkyl complex. Loss of nitrogen forms an intermediate carbene complex, which is susceptible to nucleophilic attack by an alkene. Cyclopropane production regenerates the active catalyst, Ir(TTP)CH$_3$.

Kodadek and co-workers spectroscopically observed the diazoalkyl complex formed from EDA coordination to Rh(TTP)I at temperatures below −20 °C.[36] Unlike Rh(TTP)I, Ir(TTP)CH$_3$ is an extremely active catalyst at temperatures as low as −78 °C. Consequently, intermediate diazoalkyl or carbene complexes were not observed in Ir(TTP)CH$_3$-catalyzed reactions. Additional studies were employed to further explore the catalytic mechanism for Ir(TTP)CH$_3$. Substrate competition reactions were examined to determine the olefin influence on the reaction rate (Table 4). Olefins with a broad range of steric and electronic properties were

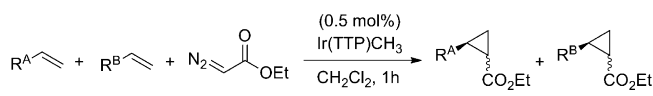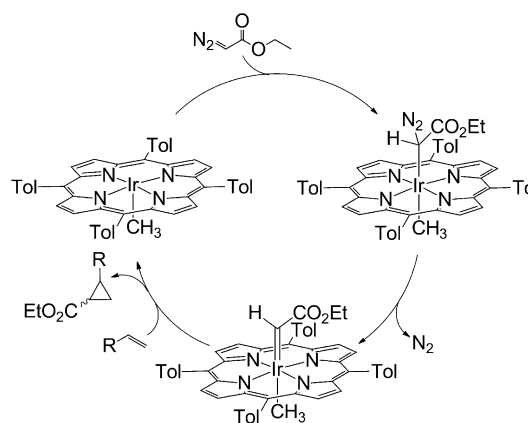**Scheme 3. Proposed General Cyclopropanation Mechanism with Ir(TTP)CH$_3$**



**Table 4. Cyclopropanation using EDA and Ir(TTP)CH$_3$: Substrate Competition Reactions**[a]



| substrate A | substrate B | ratio of A to B |
|---|---|---|
| styrene | indene | 3.9 |
| styrene | cyclohexene | only A |
| indene | cyclohexene | only A |
| 4-methylstyrene | styrene | 1.36 |
| 4-bromostyrene | styrene | 1.12 |
| 4-methoxystyrene | styrene | 1.80 |
| 4-nitrostyrene | styrene | 0.78 |
| styrene | styrene-d$_8$ | 0.85 |

[a]Conditions: $5 \times 10^{-4}$ M in Ir(TTP)CH$_3$; Ir(TTP)-CH$_3$:EDA:substrate A:substrate B = 1:200:1000:1000; reactions allowed to run for 1 h. Yields were determined by GC.

compared. Significant chemoselectivity was observed between styrene, indene, and cyclohexene. Cyclohexene was completely unreactive in the presence of either styrene or indene. For the competitive cyclopropanation of styrene and indene, products derived from styrene were favored in a ratio of 3.9:1. A comparison of para-substituted styrenes demonstrated that more electron-rich olefins reacted preferentially. A Hammett correlation with the $\sigma^+$ parameter had good linearity with $\rho^+ = -0.23$ (Figure 4). This is indicative of slight positive charge buildup in the transition state. While this $\rho^+$ value is consistent
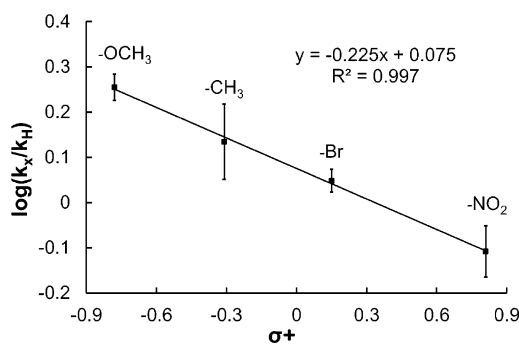


**Figure 4.** Hammett plot for the cyclopropanation of para-substituted styrenes with EDA and **1**.

    

with the mechanism in Scheme 3, it falls below the range found for iron and ruthenium porphyrin systems (−0.44 to −1.29).[20,30,37,38] In addition, the better correlation with $\sigma^+$ instead of $\sigma$ has been reported for other metalloporphyrin cyclopropanation systems.[30,37]

A secondary isotope effect was observed during the competitive cyclopropanation of styrene with styrene-$d_8$. Complex **1** exhibited an inverse isotope effect of 0.86 ± 0.03, which is comparable to that measured for iron(III) tetrakis-(pentafluorophenyl)porphyrin chloride.[20] This suggests that some olefin rehybridization occurs before the transition state of the carbene transfer step. Notably, no secondary isotope effect was observed for rhodium(III) tetramesitylporphyrin chloride.[39] In comparison to the transition state model proposed by Kodadek, Woo, and co-workers,[20] carbene transfers from iridium porphyrins have a transition state later than that for rhodium porphyrins. This implies that iridium carbene species are more tightly bound and less electropositive, which may rationalize the observed differences in diastereo- and chemoselectivity.

Despite these mechanistic insights, the rate-determining step for cyclopropanation remained unclear. Accordingly, we sought to explore the kinetics for cyclopropanation of styrene and methyl diazoacetate (MDA) in the presence of **1**. MDA was used instead of EDA to simplify monitoring the reaction by $^1$H NMR. Due to the reactivity of **1** as well as its propensity to catalyze dimerization of the diazo reagent, practical reaction conditions were not trivial to achieve. In order to monitor the reaction by NMR for several half-lives with cyclopropanation as the major product, kinetic experiments were carried out at 273.0 K, with ca. $6.4 \times 10^{-4}$ mol % of **1** and excess styrene. However, increasing the amount of styrene from 4.3 to 8.3 equiv relative to MDA reduced the rate of MDA consumption. We postulated that this inhibition was the result of competitive styrene binding to the catalyst. Indeed, on investigatation by visible absorption spectroscopy, the Soret band of **1** was red-shifted by ca. 7 nm in the presence of excess styrene, which is suggestive of olefin coordination (see the Supporting Information).

To circumvent this complication, the substrate was switched to 1-hexene. Hexene binding to **1** was considerably less substantial, as demonstrated by visible absorption spectroscopy. Unfortunately, because hexene is also less reactive than styrene, a significant amount of diazo dimerization was anticipated. Nevertheless, the cyclopropanation of hexene with MDA was studied at 273.0 K to measure the influence of catalyst, diazo reagent, and olefin concentration on reaction rate. Reactions were run with MDA as the limiting reagent, which allowed for the order of MDA to be determined using integrated rate equations. The data was plotted most suitably to the first-order rate law equation, giving a pseudo rate constant, $k'$, of (2.9 ± 0.4) $\times 10^{-4}$ s$^{-1}$ (Figure 5). In addition, the order of **1** was determined by plotting the natural log of $k'$ versus the natural log of the concentration of **1** for a series of reactions at different catalyst concentrations. The slope of the resulting line was 1.02, indicating a first-order dependence on the concentration of **1**. Reactions with different concentrations of hexene demonstrated saturation kinetics with respect to the rate of MDA consumption. The fastest rate was observed using a 2-fold excess of hexene (0.14 M) relative to MDA. At higher concentrations of hexene, the rate of MDA consumption decreased marginally, but the rate of formation of cyclopropanation products continued to increase at the expense of
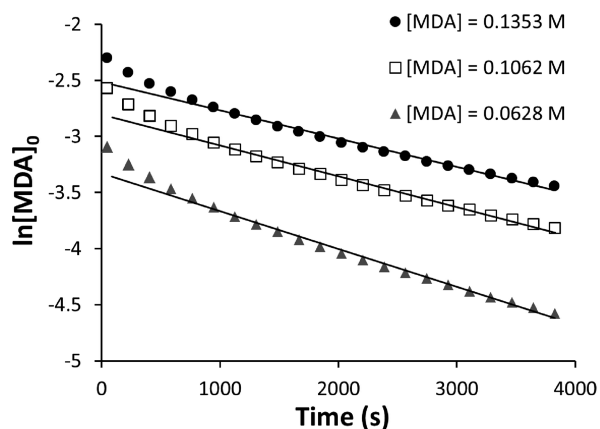


**Figure 5.** First-order integrated rate law plots at 273.0 K for different initial concentrations of MDA with 0.577 M hexene and $5.63 \times 10^{-7}$ M Ir(TTP)CH$_3$. Data points from the first 400 s were omitted in the linear regression to correct for temperature equilibration. The average slope was $(-2.9 \pm 0.4) \times 10^{-4}$ s$^{-1}$.

the dimerization products. Derivations of the rate law equations as well as initial rate data are described in the Supporting Information.

The rate dependence on the olefin concentration was further evaluated by comparing kinetic reactions in the presence and absence of 1-hexene. Three sets of reactions were run in tandem to ensure nearly equivalent conditions, and the initial rates, determined at less than 10% of reaction (before 500 s), were compared (Figure 6). The results are compiled in Table
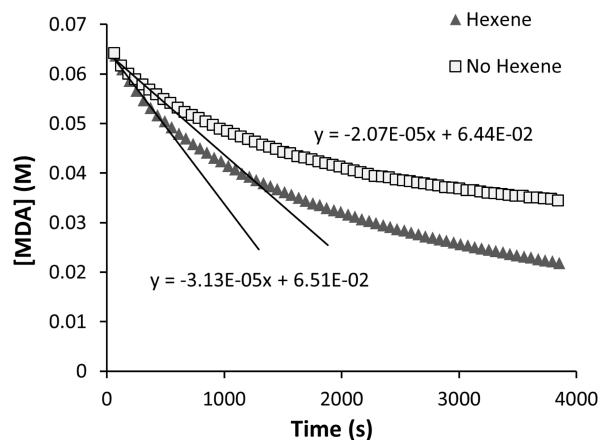


**Figure 6.** Plot of MDA consumption for the reactions of MDA and **1** at 273.0 K in the presence and absence of 1-hexene. Linear regressions were made for the data points between 0 and 500 s. The two rates shown represent the first of three sets of reactions.

S6 (Supporting Information). For each set of reactions, the initial rate of MDA consumption was 138−151% faster in the presence of hexene than in the absence of hexene. Overall, these experiments clearly demonstrate that the presence of hexene accelerated the rate of MDA consumption.

The pertinent elementary steps for metalloporphyrin-catalyzed transformations with diazo reagents are shown in Figure 7. In the analogous system using Rh(TTP)I, Kodadek and co-workers demonstrated that coordination of EDA was rapid and carbene formation was rate-limiting ($k_1, k_{-1} > k_2$).[36] For Ir(TTP)CH$_3$ catalysis, the rate-limiting step must be either carbene formation ($k_2$) or carbene transfer ($k_3, k_4$). If $k_2$ was
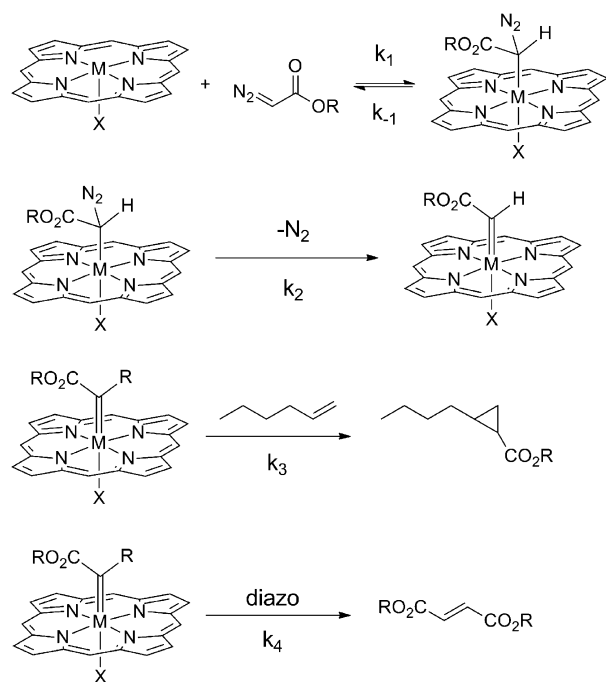
**Figure 7.** Elementary steps for the competitive cyclopropanation/dimerization of alkyl diazoacetate and 1-hexene in the presence of Ir(TTP)CH$_3$ or Rh(TTP)X.

**Scheme 4. Potential Routes for Ir(TTP)Cl(CO)-Catalyzed Cyclopropanation**



rate-limiting, the presence of hexene in the reaction would not increase the rate of MDA consumption. In fact, MDA consumption should be inhibited, because cyclopropanation would compete with the dimerization pathway and would consume only 1 equiv of MDA upon cyclopropanation. This case is not supported by the above kinetic data. Rather, the rate of MDA consumption increases in the presence of hexene, indicating that carbene transfer must be rate limiting. In other words, $k_3$ and $k_4$ are greater than $k_2$. Furthermore, since dimerization generally dominates even though hexene is present in excess, $k_4$ is likely greater than $k_3$.

In contrast to the case for **1**, the mechanism for cyclopropanation with the hexavalent iridium porphyrin complex Ir(TTP)Cl(CO) likely begins with reversible ligand dissociation to provide a vacant site for diazo coordination. Evidence supporting the formation of a heptacoordinate iridium porphyrin complex is limited and therefore seems unlikely in the present system.[40] Assuming only one ligand dissociates, two catalytic pathways are possible (Scheme 4). CO dissociation would lead to a pathway with a neutral metalloporphyrin, analogous to the mechanism proposed for Ir(TTP)CH$_3$. Alternatively, chloride dissociation to generate a formally cationic metalloporphyrin catalyst could be occurring. However, the quantitative recovery of Ir(TTP)Cl(CO) after catalysis suggests that CO dissociation is unlikely. On the other hand, comparing the cyclopropanation reactivity and selectivity of neutral (**1**) and cationic (**7**, **8**) iridium catalysts suggests that the chloride dissociation pathway may not be dominant either.

## ■ CONCLUSIONS

In summary, a variety of neutral and cationic iridium(III) porphyrin complexes were shown to be exceptionally active catalysts for the cyclopropanation of olefins with diazo compounds. Ir(TTP)CH$_3$ (**1**) was extremely robust for the conversion of EDA, producing cyclopropane TONs of 4.8 ×
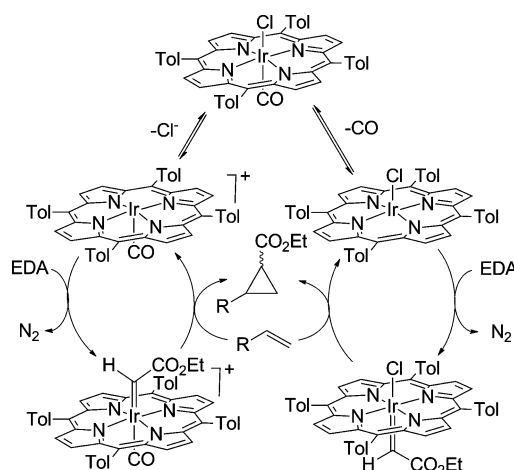
10$^5$ without significant deactivation. Cyclopropanation was explored for a variety of electronically diverse olefins. In general, electron-rich and sterically unencumbered substrates reacted the most efficiently. The cyclopropanation mechanism was explored in some depth for catalyst **1**. Competition studies using para-substituted styrenes produced a Hammett correlation with $\rho^+ = -0.23$, which indicates a buildup of positive charge in the transition state. Using styrene and styrene-$d_8$, an inverse secondary isotope effect of 0.86 ± 0.03 was observed, suggesting that moderate olefin rehybridization occurs before the transition state of the carbene transfer step. From these data, the catalytic cycle was proposed to follow a metalloporphyrin carbene pathway similar to that reported for Rh(TTP)I. However, unlike Rh(TTP)I, the rate-limiting step for catalyst **1** appeared to be carbene transfer, as determined by kinetics analyses. Similar mechanistic insights for hexacoordinate compounds were not explored, due to the ambiguity in competing pathways involving the dissociation of axial ligands. The findings presented herein indicate that significant potential exists for catalysis with iridium porphyrin complexes.

## ■ EXPERIMENTAL SECTION

All manipulations were performed under a dry nitrogen atmosphere. Ir(TTP)Cl(CO), Ir(TTP)CH$_3$, and Ir(TTP)(BF$_4$)/Ir(TTP)(CO)-(BF$_4$) were synthesized according to previously reported methods.[25,26,34] Methyl phenyldiazoacetate (MPDA) and methyl diazoacetate were prepared by procedures adapted from the literature.[41,42] All olefin substrates were dried over 4 Å molecular sieves prior to use. The styrene derivatives, except 4-nitrostyrene, were distilled and stored at −20 °C prior to use. Trimethylamine N-oxide was sublimed and stored in an inert-atmosphere glovebox. Methylene chloride and tetrahydrofuran were deoxygenated and dried by passage through columns of reduced copper and alumina. All other chemicals were purchased as reagent grade and used without further purification. NMR spectra were collected using Varian VXR 300 MHz, Varian VXR 400 MHz, or Bruker DRX 400 MHz spectrometers. Kinetic measurements were done using a Bruker DRX 400 MHz spectrometer. $^1$H NMR peak positions were referenced against residual proton resonances of deuterated solvents ($\delta$ (ppm): CDCl$_3$, 7.26; CD$_2$Cl$_2$, 5.33). Gas chromatography was performed using a Shimadzu GC-17a fitted with a HP-5 column (30 m × 0.25 $\mu$m). Ratios for kinetic isotope data were determined using a Finnegan Magnum GC-MS fitted with a HP-5 column (30 m × 0.25 $\mu$m) and a time-of-flight mass analyzer. Mesitylene was used as an internal standard for GC yield determinations. Column chromatography was performed using silica

gel (40−63 μm) purchased from Sorbent Technologies. Characterization data for the cyclopropanation products ethyl 2-phenyl-cyclopropanecarboxylate,[43] ethyl 2-methyl-2-phenylcyclopropanecarboxylate,[44] ethyl 1,1a,6,6a-tetrahydrocyclopropa[a]indene-1-carboxylate,[45] ethyl 2-butylcyclopropanecarboxylate,[44] ethyl bicyclo[4.1.0]heptane-7-carboxylate,[45] ethyl 2-methyl-3-phenylcyclopropanecarboxylate,[46] diethyl cyclopropane-1,2-dicarboxylate,[47] and methyl 1,2-diphenylcyclopropanecarboxylate[48] were previously reported. The relative stereochemistry for ethyl 2-methyl-3-phenyl-cyclopropanecarboxylate was confirmed by NOESY spectroscopy (see the Supporting Information).

**General Cyclopropanation Procedure.** The catalyst (2 μmol) was weighed as a solid and transferred to a flame-dried Schlenk flask containing a stir bar. The flask was charged with olefin substrate (1 mmol), $CH_2Cl_2$ (2.0 mL), and mesitylene (internal standard, 0.144 mmol). If the reaction was carried out at 0 or −78 °C, it was placed in an ice bath or dry ice/acetone bath, respectively. After 15 min was allowed for temperature equilibration, reagent grade EDA (0.255 mmol) was added neat, dropwise via syringe over the course of 30 s. During the reaction, aliquots were quenched with pyridine and analyzed by GC. Once the reaction was complete, volatile components were removed in vacuo. $^1H$ NMR ($CDCl_3$) was used to confirm the consumption of EDA. Cyclopropanes could be isolated by column chromatography on silica gel using hexanes and ethyl acetate (40:1) as the eluent system. Catalyst preparations varied slightly for in situ generated cationic complexes. In a glovebox, Ir(TTP)Cl(CO) (2 μmol) and excess silver tetrafluoroborate (50 μmol) were dissolved in $CH_2Cl_2$ (2 mL). The vessel was wrapped in foil and the mixture stirred at room temperature for 30 min before continuing with the above cyclopropanation protocol.

**Experiment To Measure Catalyst TON.** A dry Schlenk flask was charged with $Ir(TTP)CH_3$ ($4.13 \times 10^{-6}$ mmol) from a stock solution (1.00 mL, $4.13 \times 10^{-3}$ M) in $CH_2Cl_2$. The porphyrin solution was taken to dryness under an $N_2$ stream before styrene (7.6 mmol), mesitylene (internal standard, 0.2874 mmol), and $CH_2Cl_2$ (2.0 mL) were added. EDA (approximately 0.72 mmol) was added after the mixture was cooled to near −78 °C in an acetone/dry ice bath. The cold bath was removed after 10 min, and stirring was continued at room temperature for 50 min. An aliquot was quenched in pyridine and analyzed by GC. The reaction vessel was recooled to −78 °C, and the EDA addition was repeated. This method was repeated over the course of three EDA additions. One hour after the final addition, the reaction vessel was quenched with pyridine. Turnover numbers were measured by GC, and complete conversion of EDA was observed by $^1H$ NMR.

**General Competition Experiment.** This general method was used for all competition studies, including that with styrene-$d_8$. A $CH_2Cl_2$ stock solution (200 μL, $4.93 \times 10^{-3}$ M) of $Ir(TTP)CH_3$ (0.986 μmol) was transferred to a Schlenk flask and taken to dryness under an $N_2$ stream. Substrate A (0.987 mmol), substrate B (0.987 mmol), mesitylene (internal standard, 0.1437 mmol), and $CH_2Cl_2$ (1.0 mL) were added to the flask. The solution was allowed to equilibrate to the desired reaction temperature for 15 min. EDA (0.2 mmol) was added dropwise by syringe over the course of 30 s. After it was stirred for 1 h, the reaction mixture was quenched with pyridine and analyzed by GC.

**Setup for Kinetic Measurement Experiments.** An NMR tube was charged with **1** (ranging from $1.05 \times 10^{-4}$ to $4.20 \times 10^{-4}$ μmol) from a $5.25 \times 10^{-6}$ M $CH_2Cl_2$ stock solution and taken to dryness under reduced vacuum. The tube was taken into a glovebox and loaded with 1-hexene or styrene (ranging from 27.8 to 262 μmol) and mesitylene (2.82 μmol), and the mixture was diluted to a total volume of 420 μL with $CD_2Cl_2$. Then, the tube was fitted with a septum, cooled to 273 K, and taken to the NMR spectrometer. Spectrometer settings were prepared, including temperature equilibration to 273.0 K, prior to diazo addition. Finally, MDA (ranging from 11.6 to 56.8 umol) in a $CD_2Cl_2$ stock solution (dried over molecular sieves), which was chilled in an ice bath, was added quickly. Data collection began ca. 1 min after addition. Adding equimolar portions of MDA was challenging, despite storing the stock solution in a −20 °C freezer.

Slow volatilization of $CD_2Cl_2$ caused the MDA stock concentration to fluctuate over the course of a couple of weeks. Because MDA and all the products could be monitored during the reaction, data were normalized to the total mass balance of MDA and its products.

**$Ir(TTP)Cl(NMe_3)$ (3).** In a glovebox, Ir(TTP)Cl(CO) (34.3 mg, 0.0371 mmol) and trimethylamine N-oxide (15 mg, 0.20 mmol) were dissolved in $CH_2Cl_2$ (5 mL) and stirred at room temperature for 1 day. Volatile components were removed in vacuo. Crystals were grown by slow evaporation from $CH_2Cl_2$/MeOH and separated from solution by decanting the solvent to give **3** in 87% yield (30.8 mg, 0.0322 mmol). $^1H$ NMR ($CDCl_3$): δ 8.71 (s, 8H), 8.15 (d, $J$ = 7.2 Hz, 4H), 8.02 (d, $J$ = 7.2 Hz, 4H), 7.56 (t, $J$ = 6.0 Hz, 8H), 2.74 (s, 12H). UV−vis ($CH_2Cl_2$): $\lambda_{max}$ (log ε) 412 (5.34), 522 (4.21), 555 nm (3.47).

**$Ir(TTP)Br(CO)$ (4).** All Ir(TTP)X(CO) adducts were synthesized using the following procedure with the appropriate tetrabutylammonium salts. Halide abstraction was performed similarly to a previously reported method.[34] In a glovebox, a reaction vessel was charged with Ir(TTP)Cl(CO) (14 mg, 0.015 mmol), excess silver tetrafluoroborate (20 mg, 0.1 mmol), and $CH_2Cl_2$ (3 mL). The vessel was wrapped in foil and the mixture stirred for 2 days at ambient temperature. The resulting solids were removed by filtration. Excess tetrabutylammonium bromide (5−10 equiv) was added to the filtrate, and the mixture was stirred overnight. Aqueous workup and extraction in $CH_2Cl_2$ afforded **4** as a moderately pure red solid. Purification by column chromatography on silica gel with hexanes and $CH_2Cl_2$ (1:2) as eluent gave **4** in 54% yield (7.8 mg, $8.1 \times 10^{-3}$ mmol). X-ray-quality single crystals were grown by slow evaporation from $CH_2Cl_2$. Anal. Calcd for $C_{49}H_{36}BrIrN_4O$: C, 60.74; H, 3.74; N, 5.78. Found: C, 61.26; H, 3.81; N, 5.71. $^1H$ NMR ($CDCl_3$): δ 8.93 (s, 8H), 8.12 (t, $J$ = 7.5 Hz, 8H), 7.56 (d, $J$ = 6.0 Hz, 8H), 2.1 (s, 12H). UV−vis ($CH_2Cl_2$): $\lambda_{max}$ (log ε) 424 (5.59), 535 (4.39), 570 nm (3.88).

**$Ir(TTP)I(CO)$ (5).** Tetrabutylammonium iodide was substituted for tetrabutylammonium bromide in the procedure outlined for **4**. Ir(TTP)Cl(CO) (17.2 mg, 0.0186 mmol) led to **5** in 45% yield (8.5 mg) after column chromatography. $^1H$ NMR ($CDCl_3$): δ 8.92 (s, 8H), 8.11 (m, 8H), 7.57 (t, $J$ = 6.6 Hz, 8H), 2.71 (s, 12H). UV−vis ($CH_2Cl_2$): $\lambda_{max}$ (log ε) 422 (5.51), 533 (4.36), 569 nm (3.82).

**$Ir(TTP)(SCN)(CO)$ (6).** Tetrabutylammonium thiocyanate was substituted for tetrabutylammonium bromide in the procedure outlined for **4**. Ir(TTP)Cl(CO) (27.5 mg, 0.0297 mmol) led to **6** in 72% yield (20.2 mg). Anal. Calcd for $C_{50}H_{36}IrN_5OS \cdot ^1/_2H_2O$: C, 62.81; H, 3.90; N, 7.32. Found: C, 62.26; H, 3.34; N, 7.13. $^1H$ NMR ($CDCl_3$): δ 8.98 (s, 8H), 8.13 (dd, $J$ = 15.2 Hz, 7.6 Hz, 8H), 7.60 (t, $J$ = 6.4 Hz, 8H), 2.73 (s, 12H). UV−vis ($CH_2Cl_2$): $\lambda_{max}$ (log ε) 420 (5.59), 531 (4.42), 566 nm (3.84).

**X-ray Single-Crystal Structure Determination.** The crystal evaluation and data collection were performed at 173 K on a Bruker APEX II CCD diffractometer using Mo Kα ($\lambda$ = 0.710 73 Å). Full sphere data with 0.3° frame width were collected until a resolution of 0.74 Å. The absorption correction was based on a fit of a spherical harmonic function to the empirical transmission surface, as sampled by multiple equivalent measurements.[49] Structures were solved using direct methods and were refined in full-matrix anisotropic approximation for all non-hydrogen atoms. All hydrogen atoms were placed in the structure factor calculations at idealized positions and refined using a "riding model". The $U_{iso}$(H) values were set at 1.5 times the $U_{eq}$ value of the carrier atom. All calculations were performed using the APEX II software package.[50,51] In complexes **4** and **5**, the axial ligands were disordered by inversion and distances in these ligands were constrained during refinement.

## ■ ASSOCIATED CONTENT

### Ⓢ Supporting Information

Figures, tables, and CIF files giving Hammett plot data, kinetic isotope data, derivations of rate equations, initial rate data at different concentrations of the reagents and catalyst, the NOESY spectrum for ethyl 2-methyl-3-phenylcyclopropane-carboxylate, and complete structural data for **3**−**6**. This material is available free of charge via the Internet at http://pubs.acs.org.

CCDC 864501−864504 also contain supplementary crystallographic data for this paper. These data can be obtained free of charge from The Cambridge Crystallographic Data Centre via www.ccdc.cam.ac.uk/data_request/cif.

## ■ AUTHOR INFORMATION

**Corresponding Author**

*E-mail: kwoo@iastate.edu.

**Notes**

The authors declare no competing financial interest.

## ■ REFERENCES

(1) Che, C.-M.; Zhou, C.-Y.; Wong, E. In *Topics in Organometallic Chemistry*; Plietker, B., Ed.; Springer: Berlin/Heidelberg, Germany: 2011; Vol. 33, p 111.

(2) Lu, H.; Zhang, X. P. *Chem. Soc. Rev.* **2011**, *40*, 1899.

(3) Nicolas, I.; Le Maux, P.; Simonneaux, G. *Coord. Chem. Rev.* **2008**, *252*, 727.

(4) Davies, H. M. L.; Panaro, S. A. *Tetrahedron* **2000**, *56*, 4871.

(5) Doyle, M. P.; Duffy, R.; Ratnikov, M.; Zhou, L. *Chem. Rev.* **2010**, *110*, 704.

(6) Díaz-Requejo, M. M.; Belderrain, T. R.; Nicasio, M. C.; Perez, P. J. *Dalton Trans.* **2006**, 5559.

(7) Caballero, A.; Prieto, A.; Díaz-Requejo, M. M.; Pérez, P. J. *Eur. J. Inorg. Chem.* **2009**, *2009*, 1137.

(8) Doyle, M. P. *Angew. Chem., Int. Ed.* **2009**, *48*, 850.

(9) Ferrand, Y.; Le Maux, P.; Simonneaux, G. *Org. Lett.* **2004**, *6*, 3211.

(10) Thu, H.-Y.; Tong, G. S.-M.; Huang, J.-S.; Chan, S. L.-F.; Deng, Q.-H.; Che, C.-M. *Angew. Chem., Int. Ed. Engl.* **2008**, *47*, 9747.

(11) Hamaker, C. G.; Mirafzal, G. A.; Woo, L. K. *Organometallics* **2001**, *20*, 5171.

(12) Zhou, C.-Y.; Che, C. *Synlett* **2010**, *2010*, 2681.

(13) Che, C.-M.; Huang, J.-S. *Coord. Chem. Rev.* **2002**, *231*, 151.

(14) Xu, X.; Lu, H.; Ruppel, J. V.; Cui, X.; Lopez de Mesa, S.; Wojtas, L.; Zhang, X. P. *J. Am. Chem. Soc.* **2011**, *133*, 15292.

(15) Intrieri, D.; Caselli, A.; Gallo, E. *Eur. J. Inorg. Chem.* **2011**, *2011*, 5071.

(16) Mbuvi, H. M.; Woo, L. K. *Organometallics* **2008**, *27*, 637.

(17) Mbuvi, H.; Woo, L. K. *J. Porphyrins Phthalocyanines* **2010**, *14*, 284.

(18) Cheng, G.; Mirafzal, G. A.; Woo, L. K. *Organometallics* **2003**, *22*, 1468.

(19) Callot, H. *Tetrahedron* **1982**, *38*, 2365.

(20) Wolf, J. R.; Hamaker, C. G.; Djukic, J.-P.; Kodadek, T.; Woo, L. K. *J. Am. Chem. Soc.* **1995**, *117*, 9194.

(21) Callot, H. *Tetrahedron Lett.* **1980**, *21*, 3489.

(22) Callot, H. J.; Metz, F. *Tetrahedron Lett.* **1982**, *23*, 4321.

(23) Sadasivan, N. *J. Inorg. Nucl. Chem.* **1968**, *30*, 591.

(24) Bartley, D. W.; Kodadek, T. *J. Am. Chem. Soc.* **1993**, *115*, 1656.

(25) Ogoshi, H.; Setsune, J.; Yoshida, Z. *J. Organomet. Chem.* **1978**, *159*, 317.

(26) Yeung, S. K.; Chan, K. S. *Organometallics* **2005**, *24*, 6426.

(27) Kanchiku, S.; Suematsu, H.; Matsumoto, K.; Uchida, T.; Katsuki, T. *Angew. Chem., Int. Ed.* **2007**, *46*, 3889.

(28) Berkessel, A.; Kaiser, P.; Lex, J. *Chem. Eur. J.* **2003**, *9*, 4746.

(29) O'Malley, S.; Kodadek, T. *Tetrahedron Lett.* **1991**, *32*, 2445.

(30) Che, C.-M.; Huang, J.-S.; Lee, F.-W.; Li, Y.; Lai, T.-S.; Kwong, H.-L.; Teng, P.-F.; Lee, W.-S.; Lo, W.-C.; Peng, S.-M.; Zhou, Z.-Y. *J. Am. Chem. Soc.* **2001**, *123*, 4119.

(31) Shvo, Y.; Hazum, E. *J. Chem. Soc., Chem. Commun.* **1975**, 829.

(32) Burnett, M. N.; Johnson, C. K. *ORTEP-III: Oak Ridge Thermal Ellipsoid Plot Program for Crystal Structure Illustrations*, Oak Ridge National Laboratory Report ORNL-6895, 1996.

(33) Rohde, J. Z. *Anorg. Allg. Chem.* **1997**, *623*, 1774.

(34) Song, X.; Chan, K. S. *Organometallics* **2007**, *26*, 965.

(35) Chen, Y.; Ruppel, J. V.; Zhang, X. P. *J. Am. Chem. Soc.* **2007**, *129*, 12074.

(36) Maxwell, J.; Brown, K.; Bartley, D.; Kodadek, T. *Science* **1992**, *256*, 1544.

(37) Lai, T.-S.; Chan, F.-Y.; So, P.-K.; Ma, D.-L.; Wong, K.-Y.; Che, C.-M. *Dalton Trans.* **2006**, 4845.

(38) Galardon, E.; Le Maux, P.; Simonneaux, G. *Tetrahedron* **2000**, *56*, 615.

(39) Brown, K. C.; Kodadek, T. *J. Am. Chem. Soc.* **1992**, *114*, 8336.

(40) Cheung, C. W.; Chan, K. S. *Organometallics* **2008**, *27*, 3043.

(41) Zhao, W.-J.; Yan, M.; Huang, D.; Ji, S.-J. *Tetrahedron* **2005**, *61*, 5585.

(42) Searle, N. E. *Organic Syntheses* Wiley: New York, 1956; Collect. Vol. *36*.

(43) Chen, Y.; Fields, K. B.; Zhang, X. P. *J. Am. Chem. Soc.* **2004**, *126*, 14718.

(44) Barrett, A. G. M.; Braddock, D. C.; Lenoir, I.; Tone, H. *J. Org. Chem.* **2001**, *66*, 8260.

(45) Rosenberg, M. L.; Krivokapic, A.; Tilset, M. *Org. Lett.* **2009**, *11*, 547.

(46) Feldman, K. S.; Simpson, R. E. *J. Am. Chem. Soc.* **1989**, *111*, 4878.

(47) Doyle, M. P.; Dorow, R. L.; Tamblyn, W. H. *J. Org. Chem.* **1982**, *47*, 4059.

(48) Tarwade, V.; Liu, X.; Yan, N.; Fox, J. M. *J. Am. Chem. Soc.* **2009**, *131*, 5382.

(49) Blessing, R. *Acta Crystallogr., Sect. A* **1995**, *51*, 33.

(50) Sheldrick, G. M. *Acta Crystallogr.* **2008**, *A64*, 112.

(51) *APEX2 Version 2.2*; Bruker AXS Inc., Madison, WI, 2007.